Published in final edited form as:
J Magn Reson Imaging. 2007 November ; 26(5): 1296–1302. doi:10.1002/jmri.21141.

A Prototype RF Dosimeter for Independent Measurement of the Average Specific Absorption Rate (SAR) During MRI

John P Stralka, MS[1] and **Paul A Bottomley, PhD**[1,2,*]

1*Department of Electrical and Computer Engineering, Johns Hopkins University, Baltimore, Maryland, USA*

2*Division of MR Research, Department of Radiology, Johns Hopkins University, Baltimore, Maryland, USA*

Abstract

Purpose—To develop a scanner-independent dosimeter for measuring the average radio frequency (RF) power deposition and specific absorption rates (SAR) for human MRI exposure.

Materials and Methods—A prototype dosimeter has a transducer with orthogonal conducting loops surrounding a small signal-generating MRI sample. The loops contain resistors whose values are adjusted to load the scanner's MRI coils equivalent to an average head or body during MRI. The scanner adjusts its power output to normal levels during setup, using the MRI sample. Following calibration, the total power and average SAR deposited in the transducer are measured from the root-mean-square (rms) power induced in the transducer during MRI.

Results—A 1.5 Tesla head transducer was adjusted to elicit the same load as the average of nine adult volunteers. Once adjusted, the transducer loads other head coils the same as the head does. The dosimeter is calibrated at up to 20 W total deposited power and 4.5 W/kg SAR in the average head, with about 5% accuracy.

Conclusion—This dosimeter provides a simple portable means of measuring the power deposited in a body-equivalent sample load, independent of the scanner. Further work will develop SAR dosimetry for the torso and for higher fields.

Keywords

RF power deposition; safety; specific absorption rate; dosimetry; MRI

THERE ARE CURRENTLY over 20,000 MRI scanners performing over 60 million studies world-wide (1). About half of these scans are performed in the United States, where the number of scans has been doubling about every three years for the past decade. In the United States, over one-half of the existing scanners operate at 1.5T (2), while most luminary institutions active in medical imaging research have added 3T MRI systems, and 4T (3) and 7T (4) whole body systems are also commercially available. While MRI is not considered a significant risk (5), it is not hazard-free.

The potential for radio frequency (RF) power deposition and heating in human MRI was realized as early as 1978 (6). The mechanism for heating is the induction of eddy currents in the body by the time-dependent RF magnetic field in accordance with Faraday's Law, due to the finite conductivity of the body. Models comprised of homogeneous cylinders of tissue of measured conductivity and dielectric constant, were solved analytically for various

*Address reprint requests to: P.B., Division of MR Research, Department of Radiology, Johns Hopkins University, 601 N Caroline Street Baltimore, Maryland 21287-0843. E-mail: bottoml@mri.jhu.edu

configurations (6-8). The key results were: 1) local peak and average specific power absorption rates (SARs) in W/kg or W/cm^3 can be determined from the known RF pulse width, duty cycle, flip-angle, and sample size using relatively simple formulae (6-8); 2) SAR varies approximately quadratically with MRI frequency or field strength, and with sample radius at lower frequencies (<100 MHz); and 3) peak SAR is related to the average SAR by simple numerical factors (7). That excess RF power deposition can cause heating and burns is evidenced by voluntary reports to the U.S. Food and Drug Administration (FDA) of injuries received during clinical MRI, as summarized in Table 1 for 2005 and 2006 (9). Many of these injury reports are not linked to patient proximity to leads, metal, separate receiver coils, or the magnet bore, which may pose additional risk.

The safety of RF exposure during clinical MRI is regulated via government and industry guidelines (10,11). RF exposure is also a factor in assessing the safety of MRI in human research overseen by Institutional Review Boards (IRBs). Consequently, accurate RF dosimetry is central to the safe operation of thousands of MRI scanners and millions of human MRI scans. Indeed, issues relating to SAR are listed among the top three unsolved problems and unmet needs by each of three study groups of the International Society of Magnetic Resonance in Medicine (ISMRM) (12), underscoring the need for providing accurate and independent methods of measuring it. In Europe, the International Electrotechnical Commission (IEC) defines the whole-body SAR as the absorbed RF power (P_A in Watts) divided by patient mass (m), and the partial body SAR is calculated based on the body mass in the coil, which may be modeled by homogeneous cylinders (11). The local SAR in 1 g (9) or 10 g (11) of tissue is determined from experimentally-validated models or by experiments on phantoms (11). For homogeneous cylinders and spheres, the models yield a local SAR two to four times the average SAR (7). Heterogeneous models with quadrature excitation yield ratios of 4.5-6 for the head at 63-175 MHz (13-15), and 10-16 for male and female torsos at 1.5T and 3T (16,17). Thus, once an average SAR is determined via P_A/m, a model-based local maximum can be obtained by simple multiplication by the corresponding model factor, at least for the above frequency ranges.

One simple method of measuring SAR that satisfies the IEC guidelines and does not require MRI parameters, determines P_A from the incident (forward minus reflected) root-mean-square (rms) power P_I at the transmitter coil, but requires the coil's quality factors (Q) measured with (Q_L), and without (Q_U), the subject load (18,19). The amount of power deposited in the subject is:

$$P_A = P_I\,(1 - Q_L/Q_U)\,. \tag{1}$$

Although determining these parameters at each exam would provide a straightforward approach to measuring SAR, various expediencies are commonly adopted for reporting and limiting SAR in many commercial clinical MRI scanners. For example, the Qs and P_I are generally not measured at the coil terminals by the scanner during setup for a patient study, particularly in older scanners. Instead, fixed factory-determined parameters characterizing the selected coil-type are typically entered into scanner configuration files to calculate the SAR for a desired duty cycle, with conservative safety factors added to accommodate variations that may occur in the field. These "scanner SAR" values are utilized by the scanner for limiting pulse sequence parameters, and *are* generally accessible to the MRI operator.

The accuracy with which such "scanner SAR" values measure the true average SAR may be compromised when coil Qs and power losses in the transmit line change with time, and/or when such conservative safety factors are introduced into the scanner's SAR calculation by the manufacturer. This uncertainty is further compounded by those cases in which RF burns are sustained by patients undergoing MRI (9,20) (Table 1). Although such cases represent a tiny fraction of the millions of clinical MRI scans performed annually, they are evidence that

"scanner SAR" was incorrect, or at least not limiting, at the time of the injury. Thus, the accuracy of "scanner SARs" reported by MRI scanners today, is a concern, and in any case, the SAR is currently not verifiable independent of the scanner.

Indeed, if one seeks to independently measure deposited power via Eq. [1], access to the coil for power as well as Q_L and Q_U measurements is generally unavailable to scanner users, researchers, or medical physicists running routine checks on clinical units. Further problems arise with the testing of implanted devices, whose use in patients in need of diagnostic MRI grows exponentially. Devices that test safe at a specified "scanner SAR" level, may not be reliable if the "scanner SAR" includes unknown factors, or is scanner-dependent, as has been recently reported (21,22). A device testing as safe at a "scanner SAR" level of 4 W/kg, for example, may in fact have only been tested at, say, 2 W/kg if SAR is being conservatively overstated. In summary: 1) if patients report burning sensations during MRI (Table 1); or 2) if internal device/implant makers wish to determine that their devices are safe at a certain SAR exposure level; or 3) if questions arise during IRB assessment concerning the safe conduct of research studies, there are currently no convenient scanner-independent means of determining whether the machine is operating within regulatory SAR guidelines, other than performing thermal testing of instrumented phantoms (23).

We propose and demonstrate herein a novel prototype RF dosimeter for measuring average head or body SAR, entirely independent of the MRI scanner. Peak SAR can then be determined from average SAR by applying an appropriate model factor as above (7,13-17). The dosimeter has a transducer that is placed in the magnet during an MRI scan, from which the time-averaged SAR is read. Because the scanner automatically sets the flip-angle based on MRI signal and load, the transducer contains a small signal-generating sample which the scanner uses for setup. The sample is surrounded by resistively-loaded orthogonal conducting loops, such that the transducer provides a load to the scanner that is equivalent to the head or torso. Such a transducer can also be used for SNR measurements as described previously (24). The time-averaged (rms) RF voltage is measured across the loop loads, from which P_A and the equivalent body or head SAR are determined after calibration.

MATERIALS AND METHODS

Transducer

A prototype 1.5T SAR dosimeter transducer that is accommodated in the bore of a head coil for measuring average head SAR, is fabricated from two 18-cm square copper loops, affixed to acrylic board. The loops are oriented orthogonal to each other to permit detection of both components of a quadrature excitation field in the XY-plane, should one exist. They are tuned to the 1.5T MRI frequency, and loaded with resistors. The center of each board is removed to accommodate a small spherical $CuSO_4$-doped water phantom whose only purpose is to generate just enough MRI signal for the scanner to adjust its pulse power level and/or set up the pulse sequence flip-angles. The transducer and the circuit formed by each loop are illustrated in Fig. 1.

To determine the value of the total load resistance, R_L, for each loop such that the transducer presents a load equivalent to that of the head to the MRI scanner, Q_U and Q_L of a standard GE 1.5T Signa MRI quadrature birdcage head-coil are measured with the heads of a number of volunteers, and the average head Q_L is calulated. The head is replaced by the dosimeter's transducer, and the load resistance on the transducer is adjusted to reproduce the average head Q_L. Different head coils will, of course, have different Qs, but all that is required is that the transducer produces the same Q_L in each head coil that the average head produces. This is experimentally tested with Q measurements of different head coils. Note that the net load

resistance presented to the head coils by the transducer after calibration of R_L is greater than R_L by an amount attributable to the water phantom and other losses in the dosimeter.

Power Measurement

With the head-coil connected to the scanner and the transducer inside the MRI coil, an RF voltage with rms value V_{rms}, is induced on the transducer during MRI, in direct proportion to the input RF voltage. This can be measured with an RF oscilloscope, or a true rms RF voltmeter as exemplified in Fig. 2. The power on the head-equivalent transducer measures the total power in the head after calibration. Indeed, if power losses in the water phantom and monitoring leads are negligible, the total power deposited in the transducer loops is equal to the power deposited in the head. P_A measured in the transducer is proportional to ${V_{rms}}^2$ over the time-course of the MRI experiment.

MRI typically utilizes a pulse sequence that repeats with period T_R. This period includes short periods (~1-4 msec) during which one or more type of AM and/or FM modulated high power (≫1 kW peak) RF pulses are applied, separated by longer periods (~4-1000 msec or more) during which no RF is applied. Thus, determining V_{rms} will generally involve a measurement of the rms voltage during the i^{th} RF pulse, ${v^i}_{rms}$ and the duty cycle τ_i/T_R^i where τ_i is the width of the i^{th} RF pulse. Thus for each loop:

$$V_{rms}=\sum_i {V^i}_{rms}\tau_i/T_R^i \tag{2}$$

With the phantom in the middle of the transducer, the total power deposited in the two loops is:

$$P_A=\left[{V_{rms}}^2/R_L\right]_{\text{loop1}}+\left[{V_{rms}}^2/R_L\right]_{\text{loop2}} \tag{3}$$

where R_L is the measured total resistance of each loaded transducer loop at the RF frequency. The average SAR is then just P_A/m with m as the average head mass, in accordance with the IEC definitions (11).

However, in most cases it is prudent to calibrate the SAR dosimeter by measuring the power in the resistive load of each transducer loop as a function of the total power deposited in the dosimeter. Because R_L can have a number of values depending on the sample load it is designed to represent, it is convenient for the purpose of calibration to divide the total load resistance, R_L, into a smaller standard reference resistor, R_R, in series with a load adjusted to provide the correct Q_L, and to measure the power in R_R (Fig. 1b). This also reduces the amplitude of the peak RF voltage that must be detected. To minimize the effects of connecting cable impedance on transducer power measurements, connection cables are tuned to integral multiples of the wavelength and preferably include in-line baluns.

Calibration

The SAR dosimeter is calibrated independent of the MRI scanner, by connecting a true rms RF Wattmeter or RF voltmeter to the MRI coil input to measure P_I during excitation, with the dosimeter placed in the coil. Bench experiments with head MRI coils can use a continuous wave (cw) RF amplifier of lower power than the scanner's peak power (e.g., a few hundred Watts) but which still produces average SAR levels that are comparable to those used in MRI. Different power levels, P_I are applied to the MRI coil, and the fraction of that power deposited in the dosimeter, P_A, is determined from Eq. [1]. P_A is plotted against either ${V_{rms}}^2$ or the power measured by an rms Wattmeter in each transducer loop. The result is a linear calibration curve relating the observed power deposited in the dosimeter's load resistors, to the actual power deposited in the dosimeter in Watts. The IEC "exposed body SAR" can be derived using mean girth measurements to calculate the mean body mass enclosed by the coils for the average adult,

and dividing P_A by that, as reported previously (18). Peak SAR is obtained from the model factor relating average and peak SAR, as noted above (7,13-17). A block diagram of the complete dosimeter placed in a standard MRI "bird-cage" RF coil for calibration is depicted in Fig. 3.

Protocol for Use

The SAR dosimeter is used as follows:

1. The SAR transducer is placed in the scanner and MRI coil whose SAR is being measured, and advanced to the normal scan position. The transducer is connected to a true rms RF voltage or power measuring device (Fig. 3) outside the magnet (e.g., at the end of the patient table).
2. The scanner is started using the MRI pulse sequence for which the SAR measurement is desired, entering the average weight of the load for which the dosimeter is calibrated for, as the "patient weight."
3. The rms power is measured during MRI, and the average and/or peak SAR for the average subject is calculated using the average subject mass and average-to-peak model factor.
4. The transducer is removed and replaced by a subject for scanning.

RESULTS

To test dosimeter feasibility, Q_L and Q_U measurements are performed on nine adult coinvestigators positioned in a standard GE 1.5T head coil (baluns intact) on a metal-free bench. These data are plotted in Fig. 4. Mean Q_U was 97 ± 6. Q_L was 35 ± 6. The transducer load resistance is easily adjusted to produce the same loading. The maximum head circumference (c) and head length (chin-to-top; l) are also recorded from the group and used to estimate the average head mass exposed to the coil for the group, assuming a prolate spheroid with neutral specific gravity. This yields $m_h = lc^2/6\pi = 3.95 \pm 0.33$ kg.

To test whether, once the load is set, the transducer exerts the same loading effect as the head on different head coils with different Qs, the transducer load was set to match that of an author, and Q measurements repeated with the standard GE head coil from another 1.5T scanner, without changing the load. The results summarized in Table 2, show that although Q varies from coil-to-coil, the load presented by the dosimeter probe remains equivalent to the head used to calibrate the load (49.2 vs. 50.9; 65.5 vs. 65.0).

The setup in Fig. 3a was used to test and calibrate the dosimeter using ENI 300L and ENI MRI-2000 RF power amplifiers operating at continuous RF power levels of ≤3 W and ≤40 W rms power levels, respectively. Figure 5 details the power losses at each stage of the setup. Of a maximum of 40 W output from the MRI-2000 power amplifier, about 35W arrives at the coil, of which only about 20 W is deposited in the dosimeter's transducer, with about 17 W going into the load, R_L. The cyan curve relating the net power deposited in the dosimeter to the power deposited in R_L is used for calibration. Thus, 86% of the power attributable to the dosimeter based on the Q measurements and Eq. [1] is deposited in R_L, and the net power deposited in the head-equivalent load is 1.16 times the power measured in R_L: this is the dosimeter's calibration factor. The 3-W difference in power deposited in the transducer vs. that in R_L is attributable to losses in the water phantom and elsewhere in the transducer's loops, connectors, and structure. The measured and actual deposited power in R_L are in linear proportion to the input power. The SD of the measurements from the calibration curve is 5% (excluding two outliers), which constitutes the predicted error in using this dosimeter for measuring power. However, the scatter in the data at higher power levels here is primarily due

to instability in the RF power amplifier operating in continuous mode, and not to the dosimeter or measurement devices per se. The red curve relates the power measured in the dosimeter's reference load, to the average SAR in the m_h = 3.95 kg head on the right hand scale.

DISCUSSION

We have presented and demonstrated the feasibility of a novel SAR dosimeter for measuring the average SAR for a subject whose load it mimics, with bench measurements employing different coils and subject loading. In practice, the interaction between volume MRI coils and the scanner bore that typically alters MRI coil resonant frequencies, also necessitates that transducer tuning and final calibration be performed in the scanner or in a scanner-equivalent bore. Once calibrated for a given load and MRI frequency, the dosimeter provides SAR measurements that are independent of the MRI scanner. We are aware of no other scanner-independent SAR dosimeter devices for MRI.

Independent determinations of the deposited power using Eq. [1], require direct access to the coil ports during MRI to measure incident power, Q_L and Q_U during an exam, which is generally not feasible for scanner users and patient protocols. However, access to the bore is readily available for researchers or medical physicists performing routine safety assessment, and the proposed dosimeter is amenable to such practice since no such connections are required. The purpose of adjusting the dosimeter's load to that of the head (or body) is not to obtain measures for Eq. [1], but to ensure that the scanner applies a level of RF power during setup and MRI that is equivalent to that applied to a standard head (or body). The rms power deposited is measured directly from the transducer's loads: no other scanner measurements are required. In our case, the need for an independent SAR assessment was prompted by loss of confidence in "scanner SAR" values for setting up MRI safety evaluations of devices being developed for implantation, as well as a need to provide an independent means of assessing scanner function when investigating RF burns in an albeit small number of clinical MRI cases reported to our medical physicist. Even so, RF power deposition in MRI is far less of a risk than that posed by ionizing radiation in nuclear scanning, positron emission tomography (PET), X-ray, and computed tomography (CT), where failure to independently monitor exposure would not be an option.

While we have tested this SAR dosimeter concept with a head prototype at 1.5T, the importance of RF dosimetry increases with field and body size, upon which SAR depends approximately quadratically (6-8). Thus, at fields of 3T and higher, the IEC and FDA guidelines already limit the use of some MRI pulse sequences that are in routine clinical use at lower fields. We are planning to develop transducers for the torso, for 3T MRI, and possibly even for 7T systems, which are currently limited to research applications. Dosimeter transducers for different sized heads and torsos are also envisaged: for example, the adult head and body, the youth or infant head and body, and transducers designed for given weight ranges are conceivable. It is also possible that one dosimeter could be used for several study groups simply by applying different calibration factors. In such studies it will be important to obtain data that establishes more representative average loads for the dosimeter transducers than the limited group studied here. Finally, although we measured the power deposited in the prototype transducer with an oscilloscope, the setup envisaged is a transducer in the magnet connected to a meter that reads SAR directly (Fig. 3b). This involves incorporating the calibration factor into the meter, with allowance for the entry of different factors for different study groups.

ACKNOWLEDGMENT

Ananda Kumar helped with discussions on performing Q measurements and fabricating the transducer.

Contract grant sponsor: National Institutes of Health; Contract grant number: RR15396/EB007829.

REFERENCES

1. The Nobel Prize in Physiology or Medicine. Press Release. Oct 62003 [Last accessed: August 22, 2007]. Available at: http://nobelprize.org/nobel_prizes/medicine/laureates/2003/press.html.
2. Bottomley PA, Hart HR, Edelstein WA, et al. NMR imaging/spectroscopy system to study both anatomy and metabolism. Lancet 1983;2:273–274. [PubMed: 6135092]
3. Hardy CJ, Bottomley PA, Roemer PB, Redington RW. Rapid ^{31}P spectroscopy on a 4 Tesla whole-body system. Magn Reson Med 1988;8:104–109. [PubMed: 3173064]
4. Vaughan JT, Garwood M, Collins CM, et al. 7T vs. 4T: RF power, homogeneity, and signal-to-noise comparison in head images. Magn Reson Med 2001;46:24–30. [PubMed: 11443707]
5. Young FE, Food and Drug Administration. Fed Regist 1988;53:7575–7579.
6. Bottomley PA, Andrew ER. RF magnetic field penetration, phaseshift and power dissipation in biological tissue: Implications for NMR imaging. Phys Med Biol 1978;23:630–643. [PubMed: 704667]
7. Bottomley PA, Roemer RB. Homogeneous tissue model estimates of RF power deposition in human NMR studies. Local elevations predicted in surface coil decoupling. Ann NY Acad Sci 1992;649:144–159. [PubMed: 1580488]
8. Bottomley PA, Edelstein WA. Power deposition in whole body NMR imaging. Med Phys 1981;8:510–512. [PubMed: 7322070]
9. U.S. Food and Drug Administration. Center for Devices and Radiological Health. MAUDE data base reports of adverse events involving medical devices. [Last accessed: August 22, 2007]. Available at: http://www.accessdata.fda.gov/scripts/cdrh/cfdocs/cfMAUDE/search.CFM
10. U.S. Food & Drug Administration. Guidance for Industry and FDA Staff Criteria for Significant Risk Investigations of Magnetic Resonance Diagnostic Devices. Jul 142003 [Last accessed: August 22, 2007]. Available at: http://www.fda.gov/cdrh/ode/guidance/793.pdf
11. European Committee for Electrotechnical Standardization Central Secretariat: rue de Stassart 35, B-1050 Brussels. Particular requirements for the safety of magnetic resonance equipment for medical diagnosis (IEC 60601-2-33:2002). Available at: http://webstore.ich.ch/webstore/webstore.nsf/artnum/035706
12. Unsolved Problems and Unmet Needs in MR: Results from a survey of ISMRM Study Groups. Dec2005 [Last accessed: August 22, 2007]. Available at: http://www.ismrm.org/07/UnsolvedProblems_Results.htm
13. Collins CM, Li S, Smith MB. SAR and B1 field distributions in a heterogeneous human head model within a birdcage coil. Magn Reson Med 1998;40:847–856. [PubMed: 9840829]
14. Collins CM, Liu WZ, Wang JH, et al. Temperature and SAR calculations for a human head within volume and surface coils at 64 and 300 MHz. J Magn Reson Imaging 2004;19:650–656. [PubMed: 15112317]
15. Nguyen UD, Brown JS, Chang IA, Krycia J, Mirotznik MS. Numerical evaluation of heating of the human head due to magnetic resonance imaging. IEEE Trans Biomed Eng 2004;51:1301–1309. [PubMed: 15311814]
16. Simunic D. Calculation of energy absorption in a human body model in a homogeneous pulsed high-frequency field. Bioelectrochem Bioenerg 1998;47:221–230.
17. Liu W, Collins CM, Smith MB. Calculations of B1 distribution specific energy absorption rate and intrinsic signal-to-noise ratio for a body-size birdcage coil loaded with different human subjects at 64 and 128 MHz. Appl Magn Reson 2005;29:5–18.
18. Bottomley PA, Redington RW, Edelstein WA, Schenck JF. Estimating RF power deposition in body NMR imaging. Magn Reson Med 1985;2:336–349. [PubMed: 4094551]
19. Mansfield, P.; Morris, PG. NMR imaging in biomedicine. Academic Press; New York: 1982. p. 313
20. Dempsey MF, Condon B, Hadley DM. Investigation of the factors responsible for burns during MRI. J Magn Reson Imaging 2001;13:627–631. [PubMed: 11276109]
21. Baker KB, Tkach JA, Nyenhuis JA, et al. Evaluation of specific absorption rate as a dosimeter of MRI-related Implant Heating. J Magn Reson Imaging 2004;20:315–320. [PubMed: 15269959]

22. Baker KB, Tkach JA, Phillips M, Rezai AR. Variability in RF-induced heating of a deep brain stimulation implant across MR systems. J Magn Reson Imaging 2006;24:1236–1242. [PubMed: 17078088]

23. Bottomley, PA.; Lardo, AC.; Tully, S.; Karmarker, P.; Viohl, I. Safety and internal MRI coils. 2001 Syllabus. Special cross-specialty categorical course in diagnostic radiology: practical MR safety considerations for physicians, physicists, physicists and technologists. Radiological Society of North America; Oak Brook, IL: 2001. p. 85-90.

24. Edelstein WA, Bottomley PA, Pfeifer PM. A signal-to-noise calibration procedure for NMR imaging systems. Med Phys 1983;11:180–185. [PubMed: 6727793]

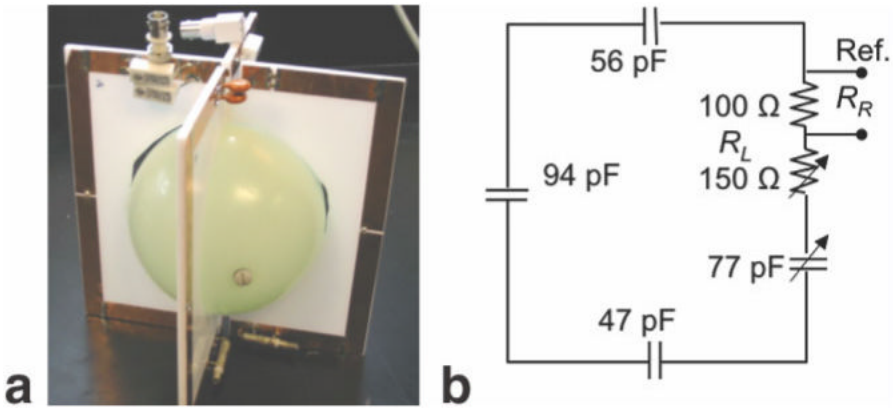

Figure 1.
Photograph (**a**) and circuit diagram for each loop (**b**) of the 1.5T head SAR dosimeter transducer. R_L is the total value of the load resistance (250 Ω) divided into a fixed reference resistor, R_R and a variable resistor used to match the Q_L of the transducer to that of the head.

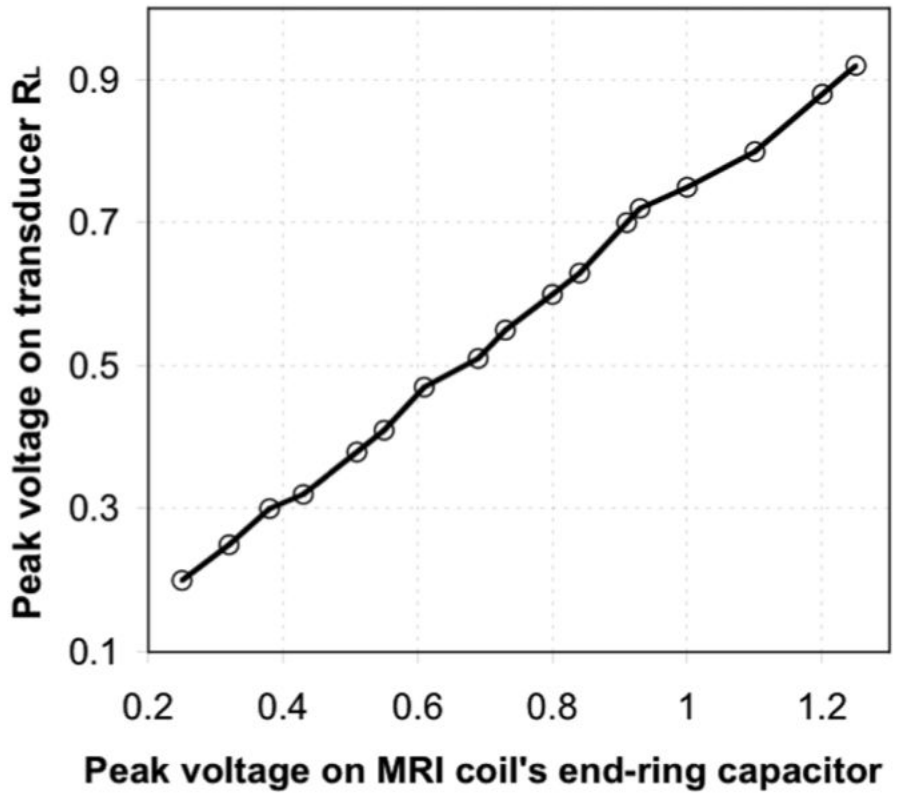

Figure 2.
Induced RF voltage measured across the loop load resistor, as a function of RF voltage applied to the MRI head coil.

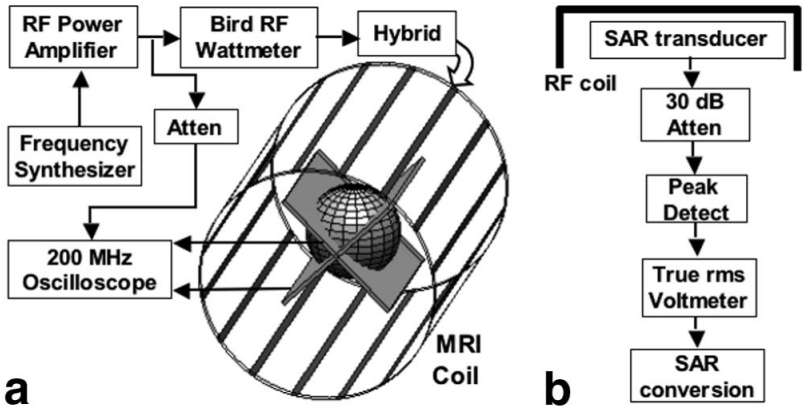

Figure 3.

a: Block diagram of the experimental setup used for calibration. The frequency synthesizer (a PTS 160) connects to an ENI MRI-2000 RF power amplifier, whose output is monitored by a Bird 4410A RF Wattmeter at the input to the quadrature hybrid on the MRI head coil. Voltage across the transducer reference resistors are monitored by a 200 MHz oscilloscope, which is also used to cross-check the input power. **b:** Block diagram of the proposed SAR dosimeter, with readout in W/kg.

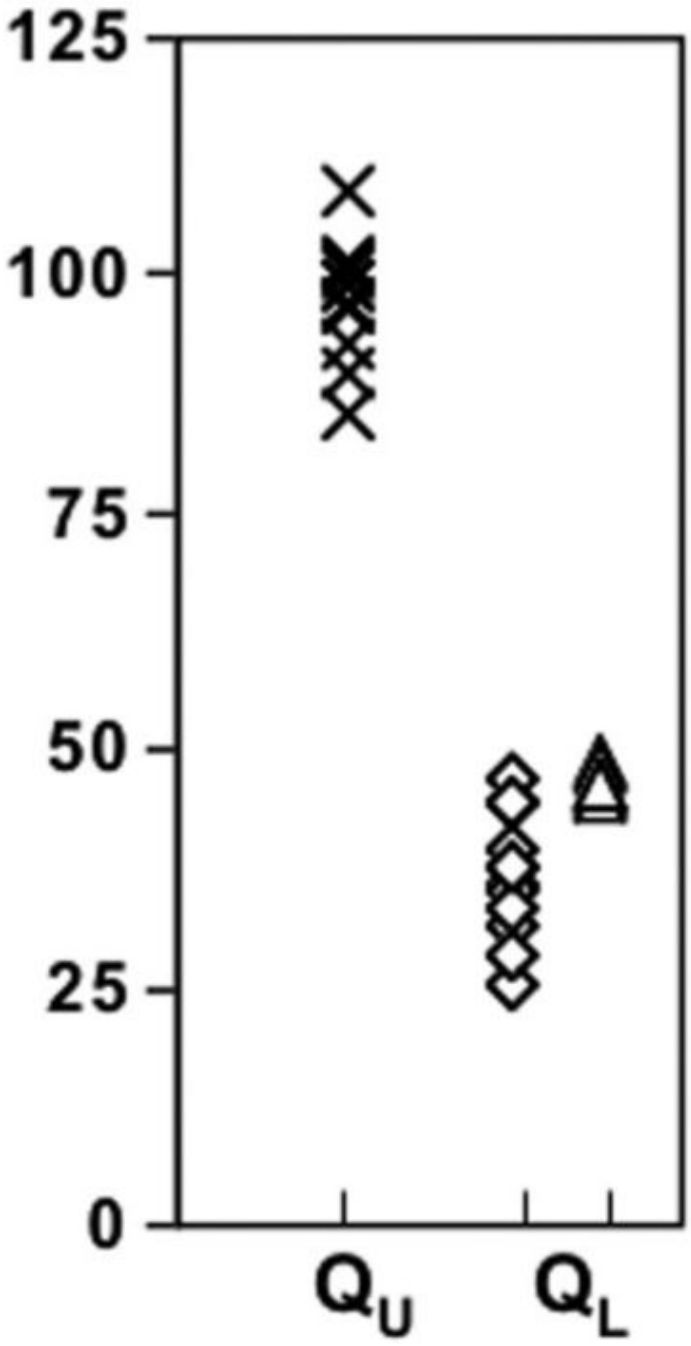

Figure 4.
Unloaded (crosses) and loaded 1.5T head coil Qs loaded with the human head (diamonds), and with the dosimeter (triangles) adjusted to provide a loaded Q equal to one of the authors for comparing the loaded Qs with the head and dosimeter in different head coils.

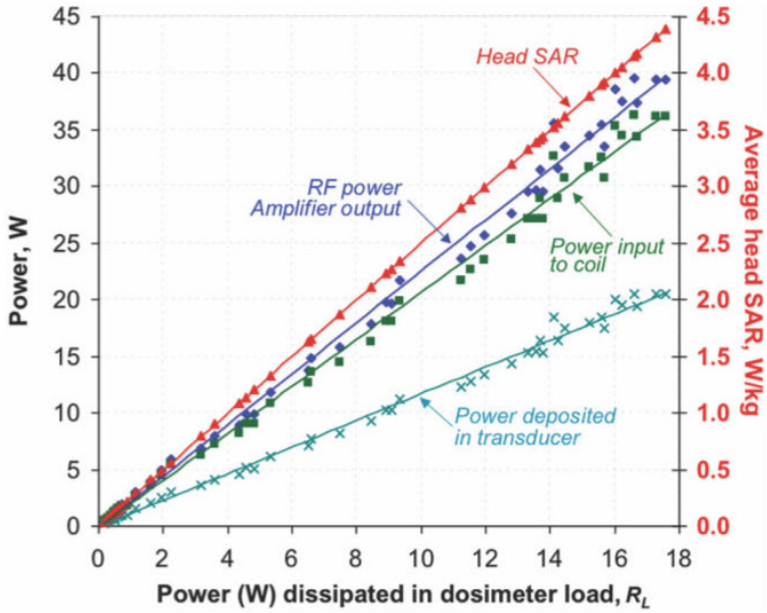

Figure 5.

Power and SAR measurements from the prototype SAR dosimeter. The measured output power from the RF amplifier (blue diamonds and line of best fit), the measured input power to the birdcage coil (incident minus reflected power; green squares and line), and the total power deposited in the transducer as deduced from Eq. [1] (cyan crosses and line), all as a function of the power measured on the dosimeter load R_L on the horizontal axis. The cyan curve relating actual-to-measured power in the dosimeter, is used for calibration. The red line (red triangles) plot the SAR (vertical axis at right) for the average head in W/kg, as a function of the power measured in R_L on the horizontal axis. [Color figure can be viewed in the online issue, which is available at www.interscience.wiley.com.]

Table 1

Adverse Events Involving RF Burns in MRI Scanners Reported to the FDA, 2005-2006*

Date of event	MRI system	Field (T)	Description	Leads[a]	Coils[b]	Bore[c]
11/17/06	GE	1.5	First degree burns/blisters, both arms, ctl coil	N	Y	N
11/17/06	GE	1.5	Burn/blisters, arm	N	N	Y
11/16/06	Philips	1.5	Burn/blister, left forearm	Y	N	N
11/2/06	GE	1.5	Burn/blister, arm	N	N	N
11/1/06	Philips	1.5	Burn/blister, arm	N	N	N
10/16/06	Philips	1.5	Burns/blisters, both thighs	N	N	N
9/15/06	GE	1.5	Second degree burn, right elbow	N	N	N
8/1/06	Hitachi	1.5	Burn, neck (ctl receive coil)	N	Y	N
7/21/06	FONAR	0.6	Third degree burns, back (no padding)	Y	N	N
7/14/06	Philips	1.5	Burns/blisters, hip	N	N	N
6/5/06	Philips	1.5	Burns/blisters, inner thighs	N	N	N
6/9/06	Philips	1.5	Second degree burns/blisters, breast	N	N	N
5/26/06	Philips	1.5	Burns/blisters, elbow, leg	N	N	N
4/29/06	Philips	1.5	Burns/blisters legs (calf)	N	N	N
3/17/06	GE	1.5	Second degree burn, elbow	N	N	Y
3/16/06	GE	1.5	Burn/blisters, hand (breast exam) injury to two patients	N	N	N
3/5/06	Philips	1.5	Second degree burns/blisters, inner thighs	N	N	N
2/23/06	Philips	1.5	Second degree burns, shoulder	N	N	N
2/13/06	GE	1.5	Burns, blisters, elbows	N	N	Y
1/24/06	Siemens	1.5	Burn/blister abdomen	N	Y	N
12/20/05	GE	1.5	Third degree burns, hands (at isocenter)	Y	N	N
12/19/05	GE	1.5	Burn/blisters, hand (breast exam)	Y	N	N
12/11/05	GE	1.5	Burn/blister, chest	N	N	N
12/10/05	GE	1.5	Second degree burns, arm, biceps	N	N	N
11/1/05	Siemens	1.5	Burn/blisters on calves	N	N	N
10/26/05	Philips	3	Second degree burn, shoulder; first degree burn, knee	N	N	N
10/13/05	GE	1.5	Second degree burn lower neck	Y	N	N
9/30/05	GE	1.5	Second degree RF burn, elbow	N	N	N
9/23/05	GE	1.5	Second degree burns (torso array coil)	N	Y	N
9/21/05	Siemens	1.5	Burns, fingers and thighs touching	N	N	N
9/14/05	GE	1.5	Burn/blister, elbow	N	N	N
8/27/05	GE	1.5	Burn/blisters, hip (8 ch body array)	N	Y	N
8/23/05	GE	1.5	Burn/blisters, hip (8 ch body array)	N	Y	Y
8/16/05	GE	1.5	Burn/blisters, hip (8 ch body array)	N	Y	N
8/15/05	Philips	1.5	Burns/blisters, elbows (head MRI)	N	N	N
7/22/05	GE	1.5	Burn, breast (lumbar MRI)	N	Y	N
6/15/05	GE		Burns/blistering on wrist (wrist coil)	N	Y	N
4/20/05	GE		Burns/blisters, C-spine exam	N	Y	N
3/17/05	GE	1.5	Burns/blisters shoulder	N	N	N
3/4/05	Philips	1.5	Burns/blister, arm (coil contact)	N	N	Y
2/14/05	GE	1.5	Burns/blisters shoulder, elbow (shoulder array)	N	Y	N
2/14/05	GE	1.5	Second degree burns, both legs (torso array)	Y	Y	N
2/7/05	Siemens	1.5	Burn/blister arm	N	N	Y

ctl = cervical-spine/thoracic/lumbar, ch = channel.

*Search term “magnetic resonance,” and screen for burns. This data is reported voluntarily, and does not represent the true incidence or distribution of such incidents (9).

[a]Report links injury to leads, including coil cables, or metal (Y = yes; N = No).

[b]Report notes use of surface coils/arrays during scan.

[c] Report notes injury was associated with bore contact.

Table 2

Coil Qs With Transducer and Head

Condition	Head coil	Measurements	
		MHz	Q
Unloaded	MRI 1	64.4	102.6 ± 0.9
	MRI 4	64.1	135.4 ± 1.1
Loaded with human head	MRI 1	63.9	49.2 ± 0.6
	MRI 4	64.0	65.5 ± 0.5
Loaded, SAR transducer	MRI 1	64.2	50.9 ± 0.4
	MRI 4	64.1	65.0 ± 0.4